THE ASTROPHYSICAL JOURNAL, 618:L33–L36, 2005 January 1

HOW PROTOSTELLAR OUTFLOWS HELP MASSIVE STARS FORM

MARK R. KRUMHOLZ
Department of Physics, University of California at Berkeley, 366 LeConte Hall, Berkeley, CA 94720; krumholz@astron.berkeley.edu
CHRISTOPHER F. MCKEE
Departments of Physics and Astronomy, University of California at Berkeley, Berkeley, CA 94720; cmckee@astron.berkeley.edu
AND
RICHARD I. KLEIN
Department of Astronomy, University of California at Berkeley, 601 Campbell Hall, Berkeley, CA 94720; and Lawrence Livermore National Laboratory, P.O. Box 808, L-23, Livermore, CA 94550; klein@astron.berkeley.edu
Received 2004 October 8; accepted 2004 November 18; published 2004 November 29

ABSTRACT

We consider the effects of an outflow on radiation escaping from the infalling envelope around a massive protostar. Using numerical radiative transfer calculations, we show that outflows with properties comparable to those observed around massive stars lead to significant anisotropy in the stellar radiation field, which greatly reduces the radiation pressure experienced by gas in the infalling envelope. This means that radiation pressure is a much less significant barrier to massive star formation than has previously been thought.

Subject headings: accretion, accretion disks — radiative transfer — stars: formation — stars: winds, outflows

Online material: color figures

1. INTRODUCTION

Stars with masses $\gtrsim 20\ M_\odot$ have short Kelvin times that enable them to reach the main sequence while they are still accreting (Shu et al. 1987). The resulting nuclear burning leads to a huge luminosity, which produces a correspondingly large radiation pressure force on dust grains suspended in the incoming gas. This force can exceed the star's gravitational pull, possibly halting accretion and setting an upper limit on the star's final mass. Early spherically symmetric calculations suggested that this phenomenon sets an upper limit on stellar masses of ~20–40 $M_\odot$ (Kahn 1974; Wolfire & Cassinelli 1987) for typical Galactic metallicities. More recent nonspherical calculations have loosened that constraint by considering the role of accretion disks (Nakano 1989; Nakano et al. 1995; Jijina & Adams 1996). Disks reduce the effects of radiation pressure by concentrating the incoming matter into a smaller solid angle, increasing its ram pressure. They also absorb stellar radiation in a thin ring and reradiate it isotropically, casting a shadow of reduced radiation pressure. Even with a disk, however, radiation pressure can still be a significant barrier to accretion. Jijina & Adams (1996) were able to form a 50 $M_\odot$ star only if it had a thin accretion disk with a radius ~4000 AU. Simulations by Yorke & Sonnhalter (2002) in two dimensions found limiting masses of ~40 $M_\odot$ before radiation pressure reversed the inflow. However, observations show that considerably more massive stars exist, and their formation mechanism remains uncertain.

Recent observations of massive protostars have added an element to this picture. Beuther et al. (2002a, 2002b, 2003, 2004) report interferometric measurements showing outflows from massive protostars with collimation factors of ~2 up to ~10. They conclude that high- and low-mass outflows have similar collimation factors, typically 2–5 (Bachiller 1996). (The collimation factor is the ratio of the outflow's length to its width.) Richer et al. (2000) show that the momentum of CO outflows driven by massive stars scales with the bolometric luminosity of the source in the same manner as for low-mass stars. From these observations, the natural conclusion is that low- and high-mass stellar outflows have a common driving mechanism and similar morphologies.

Previous theoretical work on massive star formation did not include the effects of outflows and therefore assumed that the stellar radiation either was isotropic (e.g., Jijina & Adams 1996) or had only those anisotropies induced by the presence of a disk (e.g., Yorke & Sonnhalter 2002). In this Letter, we calculate radiative transfer through dense envelopes accreting onto massive protostars, and we study the effects of outflow cavities in the envelopes on the radiation field. In § 2 we present our models for radiative transfer and for the protostellar environment. We then present the results of our calculations in § 3 and discuss conclusions in § 4.

2. MODELS

2.1. *Radiative Transfer Methodology*

We used the Monte Carlo/diffusion radiative transfer code written by Whitney et al. (2003a, 2003b) to find the temperature distribution of gas in a circumstellar envelope. The opacity comes from dust grains, which are thermally well coupled to the gas in the high-density envelope (Spitzer 1978). The grain size distribution depends on the location in the flow. The stellar spectrum is a Kurucz model atmosphere. Rather than discuss the code, grain, and stellar spectral models here, we refer readers to Whitney et al. (2003a) and to § 2.3 for a discussion of opacity in the outflow.We used 10^7 photons, sufficient to produce high signal-to-noise ratio spectra.

To calculate the radiation force on the gas, we begin with the temperature distribution determined by the Monte Carlo code. From a given position, we pick ray directions based on the HEALPix scheme (Górski et al. 1999). Along each ray, we solve the transfer equation for emission and absorption by dust grains to obtain $I_\nu(\boldsymbol{n})$, the specific intensity coming from direction $\boldsymbol{n}$. We also perform this calculation along a ray to the

star itself. Once we have found the intensity along each ray, we compute the flux

$$\boldsymbol{F}_\nu = \int I_\nu(\boldsymbol{n})\boldsymbol{n}\, d\Omega \approx \frac{4\pi}{N_{\rm rays}} \sum_{k=1}^{N_{\rm rays}} I_\nu(\boldsymbol{n}_k)\boldsymbol{n}_k, \quad (1)$$

where $N_{\rm rays}$ is the number of rays. We increase $N_{\rm rays}$ until the change in flux is less than 2.5% between iterations. We then integrate over frequency to obtain the radiation force per unit mass, $\boldsymbol{f}_{\rm rad} = c^{-1} \int \kappa_\nu \boldsymbol{F}_\nu \, d\nu$.

We ignore scattering when calculating the force (but not the temperature). Scattering of IR photons is negligible. UV and visible photons can scatter significantly, but for the fiducial envelope and star that we use, photons at the peak of the stellar spectrum are all reprocessed into IR in the inner few AU of the envelope. (In the disk the distance is vastly smaller.) Outside this layer, neglecting scattering does not change the radiation pressure force. For the same reason, the choice of stellar spectrum model is relevant only in the inner few AU of the envelope.

2.2. *Star, Disk, and Envelope Properties*

To study the effects of outflow cavities, we choose a single fiducial model for the star, disk, and envelope and vary the properties of the outflow. We place an $M_* = 50\ M_\odot$ zero-age main-sequence (ZAMS) star in a $50\ M_\odot$ envelope. The ZAMS models of Tout et al. (1996) predict a radius, surface temperature, and luminosity of $R_* = 10.8\ R_\odot$, $T_* = 4.3 \times 10^4$ K, and $L_* = 3.5 \times 10^5\ L_\odot$. McKee & Tan (2003) predict a formation time of $\sim 10^5$ yr for such a star, so we adopt an accretion rate of $\dot{M}_* = 5 \times 10^{-4}\ M_\odot\ {\rm yr}^{-1}$. The accretion luminosity is $L_{\rm acc} \approx G M_* \dot{M}_* / R_* = 7.1 \times 10^4\ L_\odot$, negligible in comparison to the central star.

Although the cores that form massive stars are probably turbulent (McKee & Tan 2003), for simplicity we adopt a simple rotationally flattened density distribution given by (Ulrich 1976; Terebey et al. 1984)

$$\rho = -\frac{\dot{M}_*}{4\pi r^2 u_r}\left[1 + 2\frac{R_{\rm cen}}{r} P_2(\cos\theta_0)\right]^{-1}, \quad (2)$$

$$u_r = -\left(\frac{2GM_*}{r}\right)^{1/2}\left(1 + \frac{\cos\theta}{\cos\theta_0}\right)^{1/2}, \quad (3)$$

$$\frac{R_{\rm cen}}{r} = \frac{\cos\theta_0 - \cos\theta}{\sin^2\theta_0 \cos\theta_0}. \quad (4)$$

Here P_2 is the Legendre polynomial, r and θ give the position in the envelope in spherical coordinates, and $R_{\rm cen}$ is the centrifugal radius of the flow. The gas at position (r, θ) was at angle θ_0 when it began falling toward the star, where θ_0 is given implicitly by equation (4). The centrifugal radius $R_{\rm cen}$ is determined by the angular momentum of material arriving at the star. When the last material in the core accretes, it is roughly $R_{\rm cen} = \beta R_{\rm core}$, where β is the ratio of the core's rotational kinetic energy to gravitational binding energy and for most cores $\beta \sim 0.02$ (Goodman et al. 1993). Since our core is half-accreted, we take $R_{\rm cen} \approx \beta R_{\rm core}/2$. We therefore adopt values of $R_{\rm core} = 0.22$ pc and $R_{\rm cen} = 400$ AU, which give the correct mass in the envelope and satisfy $R_{\rm cen} \approx \beta R_{\rm core}/2$.

In addition to the envelope, our star has a disk of radius $R_{\rm cen}$. Observations of disks around massive stars are limited, and we therefore adopt a disk mass of $M_d = M_*/10 = 5\ M_\odot$ based on the consideration that a disk more massive of the order of 10% of the central object is likely to be subject to gravitational instabilities (Shu et al. 1990) that will cause matter to accrete until marginal stability is restored. We model the disk surface density and scale height as power laws $\Sigma \propto r^{-2.25}$, $h = 0.035\,(r/R_*)$ AU. We base the choice $h \propto r$ on images from simulations of massive star formation (e.g., Yorke & Sonnhalter 2002) that show disks with little or no flaring.

2.3. *Outflow Properties*

We can partially describe the outflow cavity from observations. As discussed in § 1, high-mass outflows have collimation factors from 2 to 5, similar to low-mass stars. This corresponds to half-angles from 0 to 15°, including the uncertain inclination. We therefore test opening angles of $\theta_o = 5°$, 10° and 15°. Unfortunately, observations constrain only the asymptotic opening angle when the outflow is far from its parent core. Cavity walls from nearby low-mass sources seen in near-IR are generally curved when viewed on sufficiently small scales (e.g., Padgett et al. 1999 and Reipurth et al. 2000). This curvature is a natural result of outflow collimation by the rotationally flattened envelope (Wilkin & Stahler 1998, 2003). For massive protostars that are still embedded in dense envelopes, near-IR observations are impossible because of dust extinction. Millimeter observations, even with interferometers, are unable to probe length scales comparable to the size of the protostellar disk, at which we expect the strongest collimation and curvature. Following Whitney et al. (2003b), therefore, we parameterize the uncertain shape of the cavity as $z = a\varpi^b$, where z is the vertical distance from the star, ϖ is the distance from the outflow axis, and $a = R_{\rm core}^{1-b} \cos\theta_o / \sin^b\theta_o$ is a constant chosen to give an opening angle of θ_o at the edge of the core. We try values of $b = 1.25$, 1.5, and 2.0, coupled with a fixed wind opening angle $\theta_o = 10°$, to study the effects of variations in cavity shape. As a baseline, we also study a case with no outflow cavity.

Some gas at the outflow base will be ionized by the star's UV flux (J. T. Tan & C. F. McKee 2005, in preparation). Whether the ionized gas remains near the star depends on the outflow's structure at its base, where the density is highest and recombinations are fastest. If the outflow is ionized, it will be too hot to contain dust grains, and its opacity will come primarily from resonant scattering by metal ions (Castor et al. 1975). This is a complex subject beyond the scope of this Letter. We simply note that the opacity produced by this scattering must be far smaller than that produced by dust grains in the envelope. In the case that the outflow cavity is ionized, we may therefore set the opacity in the cavity to zero.

If the outflow is neutral, grains will reform, growing in radius $r_{\rm gr}$ at a rate (cf. Hoyle 1946)

$$\dot{r}_{\rm gr} = \alpha v_t \rho / (4\rho_{\rm gr}), \quad (5)$$

where α is the mass fraction of the element of which the grain is composed, v_t is the thermal velocity of gaseous atoms of that element, ρ is the gas density, and $\rho_{\rm gr}$ is the grain density. Growth is fastest for carbon grains, since carbon is the most abundant refractory metal in the galactic interstellar medium and has a large thermal velocity because of its low atomic mass. Sofia & Meyer (2001) estimate its mass fraction to be $\alpha_{\rm C} \approx 3 \times 10^{-3}$. Grains can only condense below the dust destruction temperature of $T_{\rm dust} \approx 1600$ K, so $v_t \lesssim 1$ km s^{-1}. The density of carbon grains is ~ 1 g cm^{-3}. For our adopted cavity shape,

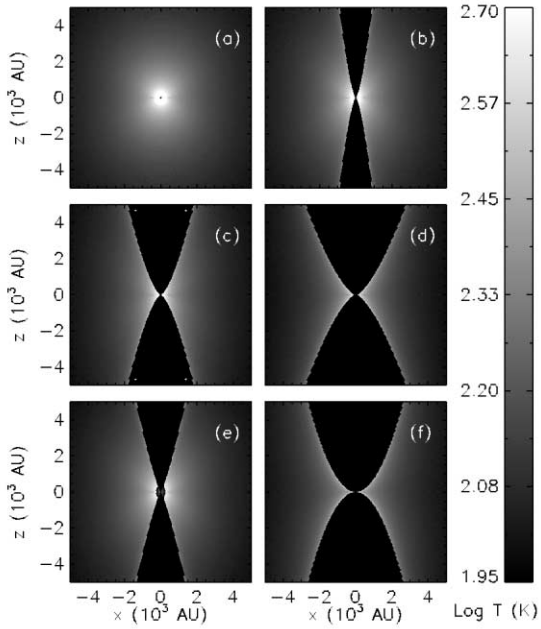

FIG. 1.—Color maps show the gas temperatures for each of our models. The models are (*a*) no wind cavity, (*b*) $\theta_o = 5°$, $b = 1.5$, (*c*) $\theta_o = 10°$, $b = 1.5$, (*d*) $\theta_o = 15°$, $b = 1.5$, (*e*) $\theta_o = 10°$, $b = 1.25$, and (*f*) $\theta_o = 10°$, $b = 2.0$. The white dots inside the cavity in panel *c* are the result of a minor code bug. [*See the electronic edition of the Journal for a color version of this figure.*]

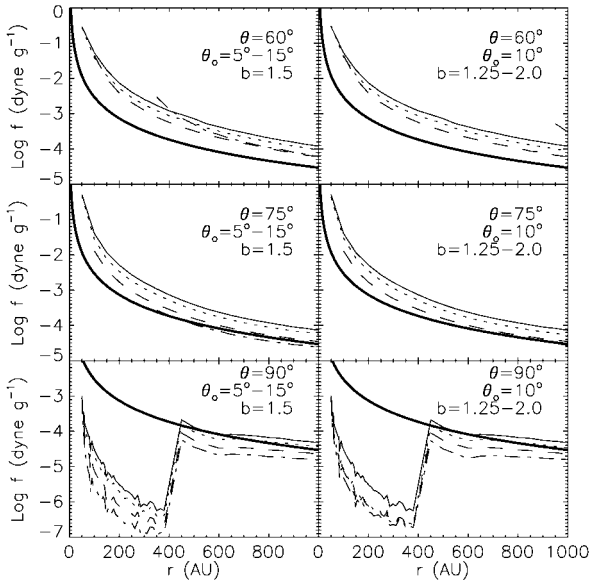

FIG. 2.—Plots show the force per unit mass due to radiation and gravity (*thick solid line*) as a function of radius, at angles of $\theta = 60°$, 75°, and 90° from the polar axis. The plots begin at the minimum value of r that is inside the infalling envelope. The three left panels show radiation with no cavity (*thin solid line*), $\theta_o = 5°$ (*dotted line*), $\theta_o = 10°$ (*dashed line*), and $\theta_o = 15°$ (*dash-dotted line*), all with $b = 1.5$. The three right panels show radiation with no cavity, $b = 1.25$ (*dotted line*), $b = 1.5$ (*dashed line*), and $b = 2.0$ (*dash-dotted line*), all with $\theta_o = 10°$. [*See the electronic edition of the Journal for a color version of this figure.*]

the wind density at a distance z from the equatorial plane must be roughly $f_w M_*/[2\pi v_w (z/a)^{2/b}]$, where v_w is the wind velocity (taken to be constant) and f_w is the fraction of mass reaching the star that is ejected into the wind. We take $f_w = 0.2$ and $v_w = v_K = (GM_*/R_*)^{1/2} \approx 1000$ km s^{-1} (Richer et al. 2000), where v_K is the Keplerian velocity at the stellar surface.

The smallest distance at which grains can form is the dust destruction radius, which we calculate to be $R_{dust} \approx 48$ AU for our fiducial model. We may therefore integrate equation (5) from R_{dust} to R_{core} to obtain the maximum size that grains can attain before escaping the core. The largest grain sizes occur for $\theta = 5°$ and $b = 1.5$, which gives $r_{gr} \leq 1.1 \times 10^{-4}$ μm; in effect, grains cannot grow past the size of molecules. In contrast, the typical grain sizes in the envelope are 0.1–0.2 μm. Stellar and envelope radiation has wavelengths $\lambda \gtrsim 2\pi r_{gr}$, so grain opacity scales as $\kappa \propto r_{gr}$. Thus, even if all the C goes into grains, the opacity in the outflow is smaller than that in the envelope by at least a factor of ~800. If we included cooling of the outflow and evaluated the grain size at radii smaller than R_{core}, the reduction would be even larger. We conclude, therefore, that dust opacity in a neutral outflow is negligible in comparison to the opacity in the infalling envelope. Since for either a neutral or an ionized outflow the opacity is negligible, we set the opacity in the outflow cavity to zero in our calculations.

3. RESULTS AND DISCUSSION

We show the gas temperature distribution for each of our models in Figure 1. Although our core extends to 0.22 pc, we concentrate on the inner few thousand AU, where the radiation pressure force is strongest. The plot shows that in models with a cavity, the gas is hotter on the inside edge of the outflow cavity but is cooler elsewhere. Since because of rotational flattening most of the gas is attempting to accrete close to the equatorial plane, this means that the bulk of the accreting gas is cooler in runs with an outflow. The effect is stronger for outflow cavities with larger opening angles and for cavities that are wider at their base.

We show the radiation pressure force versus radius at angles of $\theta = 60°$, 75°, and 90° from the pole in Figure 2. Consistent with the reduced temperature, the radiation pressure force is also substantially smaller in runs with an outflow cavity. For our "intermediate" model with $\theta_o = 10°$, $b = 1.5$, the radiation pressure force is smaller than in the run with no cavity by a factor of up to 4.6. For the other runs, the peak reductions in radiation force were a factor of 1.7 ($\theta_o = 5°$, $b = 1.5$), 14.4 ($\theta_o = 15°$, $b = 1.5$), 4.2 ($\theta_o = 10°$, $b = 1.25$), and 7.2 ($\theta_o = 10°$, $b = 2.0$). Thus, the amount by which the wind cavity reduces radiation pressure shows moderate dependence on the wind curvature and opening angle, but for only one combination of parameters was the reduction less than a factor of 4. Comparing radiation and gravitational forces, it is clear that this reduction can mean the difference between accretion halting or continuing.

To check how the results depend on properties of the envelope, which has a comparatively low surface density compared to most high-mass cores, we reran the intermediate and no cavity cases with identical R_{cen} and R_{core} but a 100 $M_\odot$ envelope. The case with no wind cavity showed little change in force with envelope mass. With a cavity, the increased envelope mass decreased the radiation pressure force at equatorial angles so that radiation was stronger than gravity only at $\theta \lesssim 60°$, increasing the fraction of solid angle through which accretion could occur. Thus, our results likely represent a *lower limit* on the reduction in radiation pressure force that outflow cavities actually produce.

To determine how the effect of the cavity compares to that

produced by the disk and the rotationally flattened envelope alone, we also considered a spherical envelope, with no cavity, no disk, and $R_{\rm cen} = 0$ in equations (2)–(4). We compared this to the run with our fiducial disk and envelope parameters and no cavity. At angles $\gtrsim 75°$, the radiation pressure force in the spherical case was a factor of a few higher, while at angles $\lesssim 60°$ it was comparable or smaller. Thus, our intermediate wind cavity reduces the radiation pressure force relative to the disk-and-envelope–only case by about the same amount that the disk-and-envelope case reduces it relative to purely spherical. Collimation of the radiation field by the disk and envelope and collimation by the outflow cavity are about equally important and reinforce each other. Together, they reduce the radiation pressure force in the intermediate cavity case by a factor of ~ 10 relative to what one would find for an isotropic radiation field.

In all our tests, the degree of radiation collimation is roughly consistent with expectations. J. T. Tan & C. F. McKee (2005, in preparation) show that the fraction of radiation escaping an envelope through a path of optical density τ is proportional to $(1 + \tau)^{-1}$. In our case, the flux fraction escaping from the core at angles between θ and $\theta + d\theta$ should roughly satisfy

$$dF(\theta) \propto [1 + \tau(\theta)]^{-1} d[\cos(\theta)], \quad (6)$$

where $\tau(\theta)$ is the optical depth at angle θ. There is considerable uncertainty in applying this to our problem because $\tau(\theta)$ is frequency-dependent. However, if we use the Rosseland mean opacity at $T_{\rm dust} = 1600$ K, then at most angles equation (6) predicts roughly the correct flux fraction.

4. CONCLUSION

We have shown that an outflow can substantially change the radiation field and radiation pressure around a massive protostar. The outflow cavity provides an optically thin channel through which radiation can escape, significantly reducing the radiation pressure. With no wind cavity, in our fiducial model the radiation pressure force is stronger than gravity essentially everywhere except inside the accretion disk, and it is therefore likely that accretion would be halted. In our intermediate model, outside the centrifugal radius radiation is weaker than gravity over about π steradians, providing a large funnel through which accretion can continue. The calculation that we have performed here is only a proof of principle, and we are currently performing three-dimensional radiation hydrodynamic adaptive mesh refinement simulations. Our results strongly argue, however, that the presence of outflows provides a mechanism for circumventing the radiation pressure limit to protostellar accretion. Surprisingly, outflows that drive gas out of a collapsing envelope may increase rather than decrease the size of the final massive star.

We thank Jonathan Tan for useful discussions. This work was supported by NASA GSRP grant NGT 2-52278 (M. R. K.), NSF grant AST 00-98365 (C. F. M.), NASA ATP grant NAG5-12042 (R. I. K. and C. F. M.), and the US Department of Energy at the Lawrence Livermore National Laboratory under the auspices of contract W-7405-Eng-48 (R. I. K.).

REFERENCES

Bachiller, R. 1996, ARA&A, 34, 111
Beuther, H., Schilke, P., & Gueth, F. 2004, ApJ, 608, 330
Beuther, H., Schilke, P., Sridharan, T. K., Menten, K. M., Walmsley, C. M., & Wyrowski, F. 2002a, A&A, 387, 931
Beuther, H., Schilke, P., & Stanke, T. 2003, A&A, 408, 601
Beuther, H., Walsh, A., Schilke, P., Sridharan, T. K., Menten, K. M., & Wyrowski, F. 2002b, A&A, 390, 289
Castor, J. I., Abbott, D. C., & Klein, R. I. 1975, ApJ, 195, 157
Goodman, A. A., Benson, P. J., Fuller, G. A., & Myers, P. C. 1993, ApJ, 406, 528
Górski, K. M., Hivon, E., & Wandelt, B. D. 1999, in Evolution of Large Scale Structure, ed. A. J. Banday, R. S. Sheth, & L. A. N. da Costa (Enschede: PrintPartners Ipskamp), 37
Hoyle, F. 1946, MNRAS, 106, 406
Jijina, J., & Adams, F. C. 1996, ApJ, 462, 874
Kahn, F. D. 1974, A&A, 37, 149
McKee, C. F., & Tan, J. T. 2003, ApJ, 585, 850
Nakano, T. 1989, ApJ, 345, 464
Nakano, T., Hasegawa, T., & Norman, C. 1995, ApJ, 450, 183
Padgett, D. L., Brandner, W., Stapelfeldt, K. R., Strom, S. E., Terebey, S., & Koerner, D. 1999, AJ, 117, 1490
Reipurth, B., Yu, K. C., Heathcote, S., Bally, J., & Rodríguez, L. F. 2000, AJ, 120, 1449
Richer, J. S., Shepherd, D. S., Cabrit, S., Bachiller, R., & Churchwell, E. 2000, in Protostars and Planets IV, ed. V. Mannings, A. P. Boss, & S. S. Russell (Tucson: Univ. Arizona Press), 867
Sofia, U. J., & Meyer, D. M. 2001, ApJ, 554, L221
Spitzer, L. 1978, in Physical Processes in the Interstellar Medium (New York: Wiley), 191
Shu, F. H., Adams, F. C., & Lizano, S. 1987, ARA&A, 25, 23
Shu, F. H., Tremaine, S., Adams, F. C., & Ruden, S. P. 1990, ApJ, 358, 495
Terebey, S., Shu, F. H., & Cassen, P. 1984, ApJ, 286, 529
Tout, C. A., Pols, O. R., Eggleton, P. P., & Han, Z. 1996, MNRAS, 281, 257
Ulrich, R. K. 1976, ApJ, 210, 377
Whitney, B. A., Wood, K., Bjorkman, J. E., & Cohen, M. 2003a, ApJ, 598, 1079
Whitney, B. A., Wood, K., Bjorkman, J. E., & Wolff, M. J. 2003b, ApJ, 591, 1049
Wilkin, F. P., & Stahler, S. W. 1998, ApJ, 502, 661
———. 2003, ApJ, 590, 917
Wolfire, M. G., & Cassinelli, J. P. 1987, ApJ, 319, 850
Yorke, H. W., & Sonnhalter, C. 2002, ApJ, 569, 846